Supporting Information

Photocatalytic Syngas Production using Conjugated Organic Polymers

Zhiwei Fu,[a] Anastasia Vogel,[a] Martijn A. Zwijnenburg,[b] Andrew I. Cooper,[*,a] and Reiner Sebastian Sprick[*,a,c]

[a] *Department of Chemistry and Materials Innovation Factory, University of Liverpool, 51 Oxford Street, Liverpool L7 3NY, UK. Email: aicooper@liverpool.ac.uk*

[b] *Department of Chemistry, University College London, 20 Gordon Street, London WC1H 0AJ, UK.*

[c] *Department of Pure and Applied Chemistry, University of Strathclyde, Thomas Graham Building, 295 Cathedral Street, Glasgow G1 1XL, UK. Email: sebastian.sprick@strath.ac.uk*

Fourier-transform infrared spectroscopy

Transmission FT-IR spectra were recorded on a Bruker Tensor 27 at room temperature; samples were prepared as pressed KBr pellets and analyzed for 16 scans with a resolution of 4 cm^{-1}.

UV-Vis Measurements

UV-Visible absorption spectra of all polymers were collected on an Agilent Cary 5000 UV-Vis-NIR Spectrometer by measuring the reflectance of powders in the solid-state.

Scanning electron microscopy

The morphology of the polymers was performed using a Hitachi S-4800 cold field emission scanning electron microscope (FE-SEM). On Hitachi M4 aluminium stubs, samples were treated by depositing the powders with an adhesive high-purity carbon tab.

Scanning Transmission Electron Microscope

STEM images were obtained on a Tescan S8000G with a TEM detector. Images were recorded at 20 KeV with a current of 125 pA. All images were recorded in both epifluorescent (EF) mode and High Angle Dark Field (HADF) mode.

Inductively coupled plasma - optical emission spectrometry (ICP-OES) analysis

Before measuring, all samples were digested in nitric acid (67–69%, trace metal analysis grade) with a microwave using an in-house procedure. The solutions were diluted with water before the measurement by Spectro Ciros ICP-OES and the instrument was calibrated with standards in aqueous solution.

Time-correlated single photon counting (TCSPC) measurements

TCSPC experiments were obtained on an Edinburgh Instruments LS980-D2S2-STM spectrometer equipped with picosecond pulsed LED excitation sources and a R928 detector. Suspensions were treated by ultrasonicating the materials in acetonitrile or acetonitrile water and triethanolamine (3/1/1) solution purged with N_2 or CO_2. The instrument response was collected with colloidal silica (LUDOX® HS-40, Sigma-Aldrich) at the excitation wavelength without any filter. Decay times were fitted in the FAST software employing suggested lifetime estimates.

Transmission and backscattering experiments

All the data were collected on a Formulaction S.A.S. Turbiscan AGS with an 880 nm NIR diode and a detector at 180° or 45° (relative to the light source) in a cylindrical glass cell. Samples were dispersed in 20 mL acetonitrile, water and triethanolamine mixture (v/v/v=3/1/1) and sonicated for 15 minutes before measurement. Then, the transmission and backscattering of the suspensions were measured in cylindrical glass cells from 5000 to 30,000 μm every 40 μm.

(TD-)DFT Calculations

The potentials of the charge carriers and exciton in P74 and those of the solution reactions involving TEOA were calculated using our standard approach[1,2] using the B3LYP[3–5] density-functional, the DZDP[6] basis-set and the COSMO[7] solvation model (ε_r 80.1). The calculation[8] of the solution potential is based on free-energies at 298.15 K and involves a standard-state correction, such that the standard-state for all soluble species is 1 mol/L, except for liquid water, where the standard-state is 55.4 mol L^{-1}. All calculations were performed using Turbomole 7.01 and employed the m3 integration grid and standard convergence criteria.

Table S-1. Evolution rates of gaseous products for high-throughput screening polymer photocatalysts.

Photocatalyst	H_2 Evolution rate (μmol g^{-1} h^{-1})[a]	CO Evolution rate (μmol g^{-1} h^{-1})[a]	CO selectivity (%)[b]
Blank	-[c]	0.8 ± 0.6	-[c]
***p*-Sexiphenylene**	1.0 ± 0.9	1.0 ± 0.6	50.0
P1S	129.8 ± 0.6	77.7 ± 3.5	37.4
P1K	30.3 ± 0.8	189.7 ± 6.3	86.2
P4	207.4 ± 6.7	291.9 ± 8.0	58.5
P7	1523.7 ± 104.0	959.1 ± 26.3	38.6
P10S	2676.3 ± 213.6	839.7 ± 188.7	23.9
P10Y	321.6 ± 28.0	172.4 ± 2.2	34.9
P29	351.0 ± 150.9	276.9 ± 100.4	44.1
P30	115.9 ± 51.0	68.8 ± 15.0	37.2
P31	12.3 ± 0.4	6.1 ± 1.7	33.0
P74	-[c]	0.3 ± 0.1	-[c]

[a] Average of two runs. Conditions: polymers (5 mg), $CoCl_2$ (1 μmol), 2,2'-biyridine (2 mg) solvent (4 mL, MeCN / H_2O=3:1), TEOA (1 mL), solar simulator (5 h), GC-TCD Headspace; [b] $Selectivity = \frac{n_{CO}}{(n_{CO} + n_{H_2})} \times 100\%$; [c] Not detected.

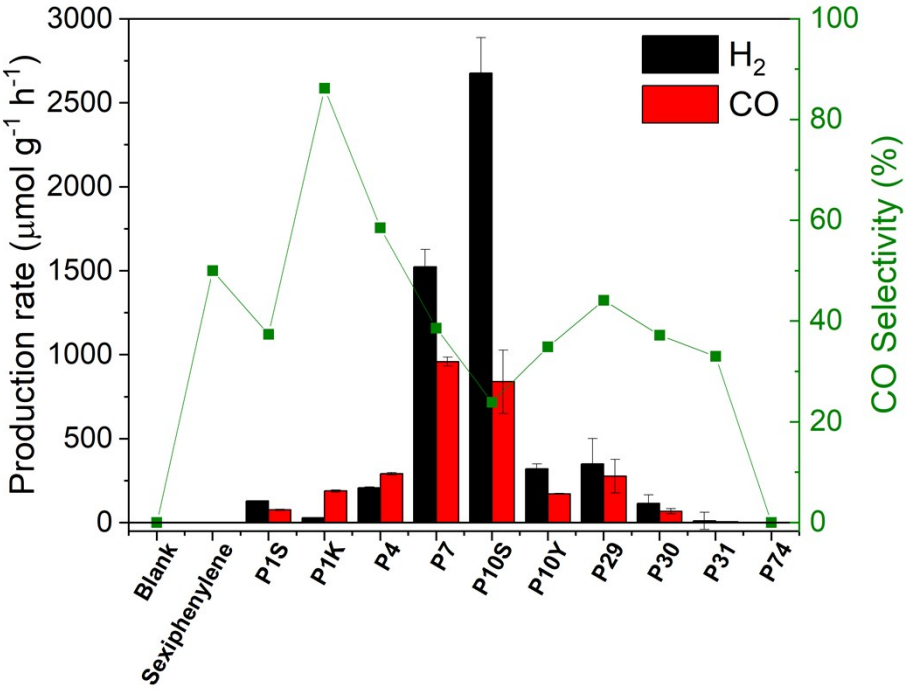

Figure S-1. Gas evolution rates and selectivity of gaseous products produced by all photocatalysts in the high-throughput screening experiment. Conditions: polymers (5 mg), $CoCl_2$ (1 μmol), 2,2'-biyridine (2 mg) solvent (4 mL, MeCN / H_2O=3:1), TEOA (1 mL), solar simulator (5 hours).

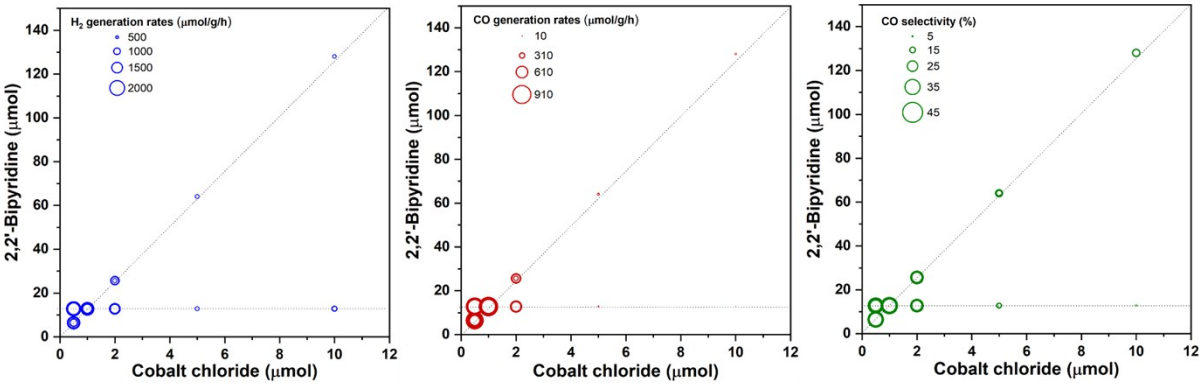

Figure S-2. Evolution rates of gaseous products and CO selectivity of P7 with of $CoCl_2$ and bpy. Conditions: P7 (5 mg, 0.155 wt. % Pd), solvent (4 mL, MeCN / H_2O=3:1), TEOA (1 mL), solar simulator (5 hours).

Table S-2. Gas evolution rates of gaseous products of P7 with of $CoCl_2$ and bpy at a constant relative ratio.

Entry	$CoCl_2$ (µmol)	Bpy (mg)	H_2 Production rate (µmol g^{-1} h^{-1})	CO Production rate (µmol g^{-1} h^{-1})	Selectivity for CO production (%)	$n(H_2)$: $n(CO)$
1[a]	0.5	1	1403.6 ± 284.3	738.3 ± 117.3	34.5	1.9 : 1
2[a]	1	2	1307.3 ± 457.4	642.7 ± 150.1	33.0	2.0 :1
3[a]	2	4	928.9 ± 270.7	381.7 ± 123.4	29.1	2.4 : 1
4[a]	5	10	604.6 ± 16.8	114.7 ± 20.4	15.9	5.3 : 1
5[a]	10	20	528.0 ± 10.9	104.1 ± 15.9	16.5	5.1 : 1

[a] Conditions: P7 (5 mg, 0.155 wt. % Pd), solvent (4 mL, MeCN / H_2O=3:1), TEOA (1 mL), CO_2 atmosphere, solar simulator (5 hours).

Table S-3. Gas evolution rates of gaseous products of P7 with of $CoCl_2$ and bpy with a varied relative ratio.

Entry	$CoCl_2$ (μmol)	Bpy (mg)	H_2 Production rate (μmol g^{-1} h^{-1})	CO Production rate (μmol g^{-1} h^{-1})	Selectivity for CO production (%)	$n(H_2)$: $n(CO)$
1[a]	0.5	2	1686.6 ± 238.9	805.5 ± 45.9	32.3	2.1 : 1
2[a]	1	2	1558.4 ± 102.3	900.3 ± 27.4	36.6	1.7 : 1
3[a]	2	2	1338.7 ± 139.8	543.8 ± 36.3	28.9	2.5 : 1
4[a]	5	2	607.9 ± 4.4	85.1 ± 8.7	12.3	7.1 : 1
5[a]	10	2	739.8 ± 34.8	37.8 ± 6.3	4.9	19.6 : 1

[a] Conditions: P7 (5 mg, 0.155 wt. % Pd), solvent (4 mL, MeCN / H_2O=3:1), TEOA (1 mL), CO_2 atmosphere, solar simulator (5 hours) .

Table S-4. Gas evolution rates of gaseous products of blank experiments with of $CoCl_2$ and bpy.

Entry	$CoCl_2$ (µmol)	Bpy (mg)		H_2 Production rate (µmol g^{-1} h^{-1})	CO Production rate (µmol g^{-1} h^{-1})
1[a]	0.5	1		-[b]	0.4 ± 0.01
2[a]	1	2		-[b]	0.3 ± 0.01
3[a]	2	4	constant ratio of $CoCl_2$/Bpy	-[b]	0.25 ± 0.05
4[a]	5	10		-[b]	0.2 ± 0.01
5[a]	10	20		-[b]	0.3 ± 0.01
6[a]	0.5	2		-[b]	0.25 ± 0.05
7[a]	1	2		-[b]	0.3 ± 0.01
8[a]	2	2	varied ratio $CoCl_2$/Bpy	-[b]	0.3 ± 0.01
9[a]	5	2		-[b]	0.25 ± 0.05
10[a]	10	2		-[b]	0.3 ± 0.01

[a] Conditions: solvent (4 mL, MeCN / H_2O=3:1), TEOA (1 mL), CO_2 atmosphere, solar simulator (5 hours); [b] Not detected.

Table S-5. P7 synthesized with various palladium loadings.

Materials	Amount of $[Pd(PPh_3)_4]$ used in polymerisation[a]	Yield / %	Residual Pd[b] / wt %
P7-0.1%	0.1 mol% (2.3 mg)	75	0.043
P7-0.5%	0.5 mol% (11.6 mg)	99	0.073
P7-1%	1 mol% (23 mg)	Quant.	0.237
P7-2%	2 mol% (46.2 mg)	Quant.	0.504
P7-3%	3 mol% (69.3 mg)	Quant.	0.769
P7-5%	5 mol% (115.6 mg)	Quant.	1.444

[a] 3,7-Dibromodibenzo[*b*,*d*]thiophene sulfone (0.748 g, 2.0 mmol), 1,4-benzene diboronic acid (0.331 g, 2.0 mmol), *N*,*N*-dimethylformamide (40 mL) and K_2CO_3 (aqueous, 2.0 M, 8 mL) were used in this reaction; [b] The amount of residual palladium in the material as measured via ICP-OES.

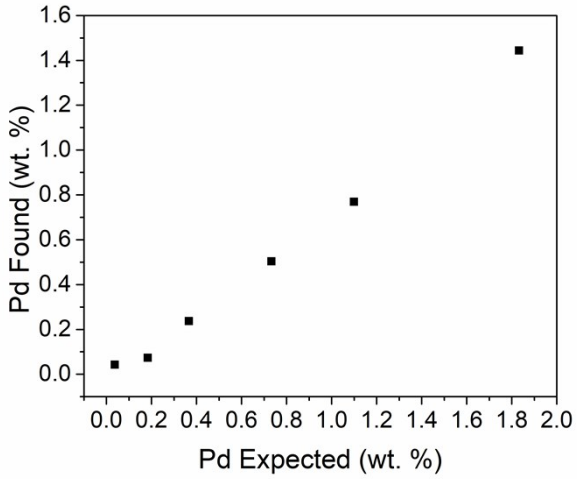

Figure S-3. Expected and measured palladium content of P7 synthesised with different amouts of $[Pd(PPh_3)_4]$.

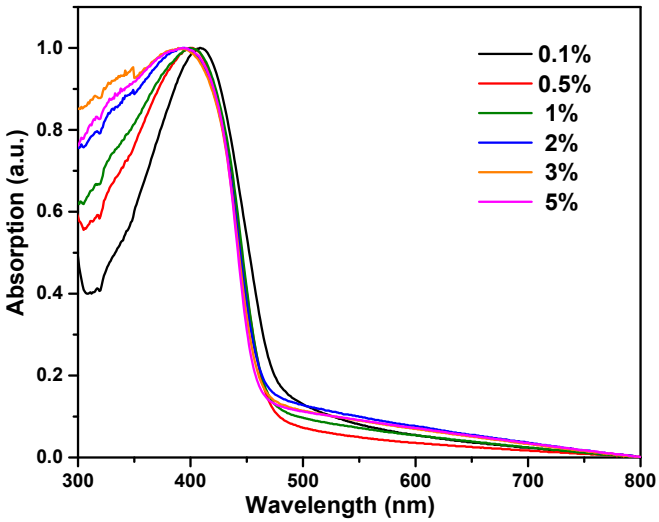

Figure S-4. UV-vis spectra of P7 synthesised with different amouts of $[Pd(PPh_3)_4]$.

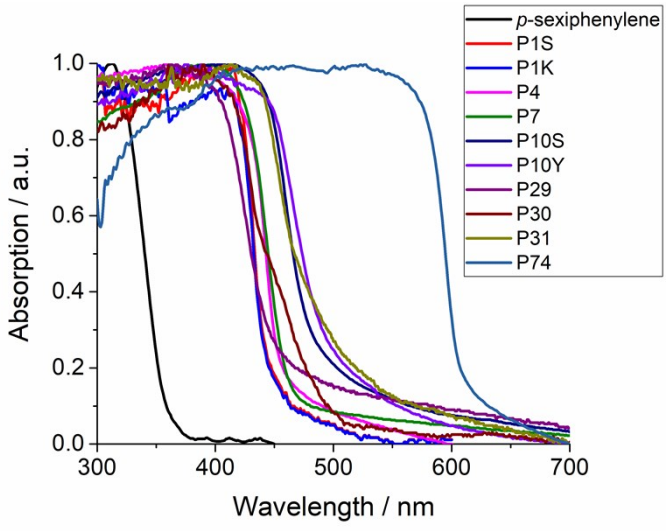

Figure S-5. UV-Vis Spectra of all photocatalysts in this study measured in the solid-state.

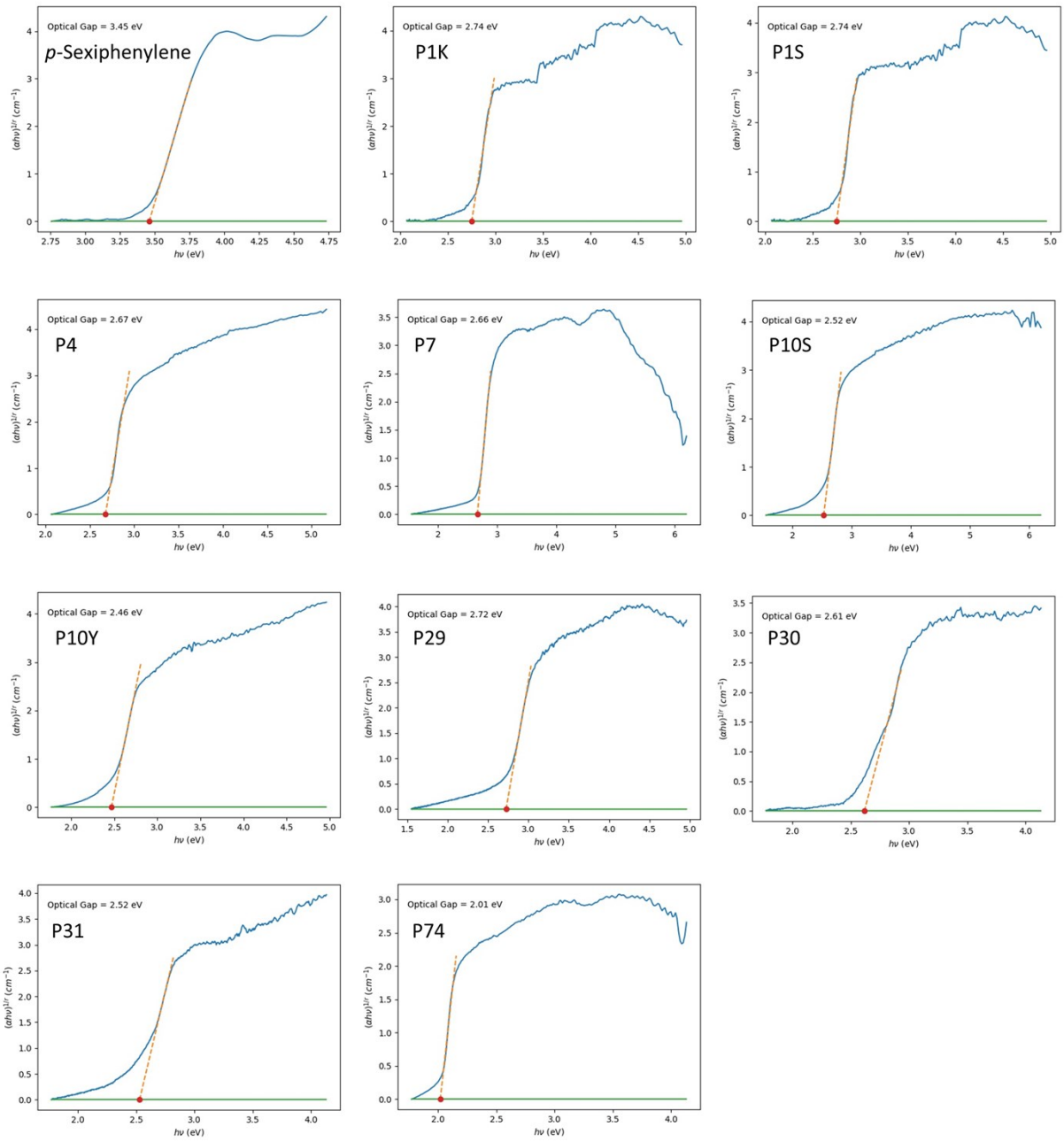

Figure S-6. Tauc plots for all photocatalysts in this study.

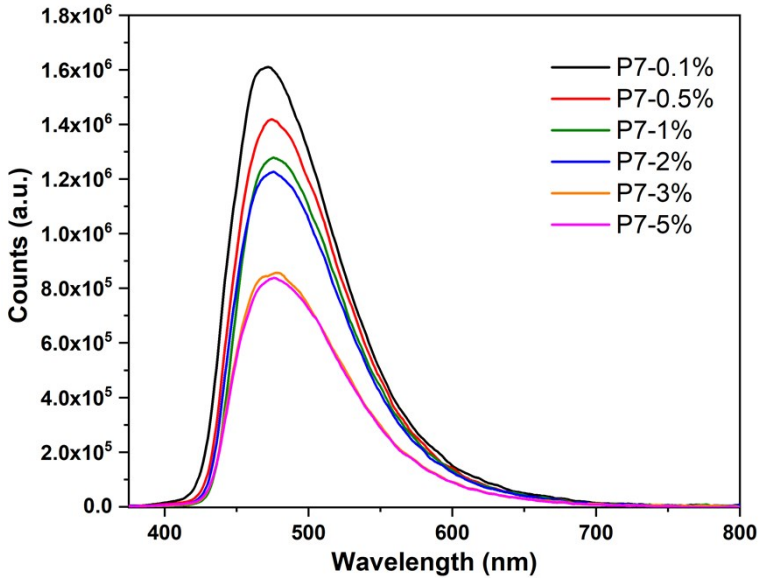

Figure S-7. Photoluminescence spectra (λ_{exc} = 370 nm) of P7 synthesized with different amouts of [$Pd(PPh_3)_4$].

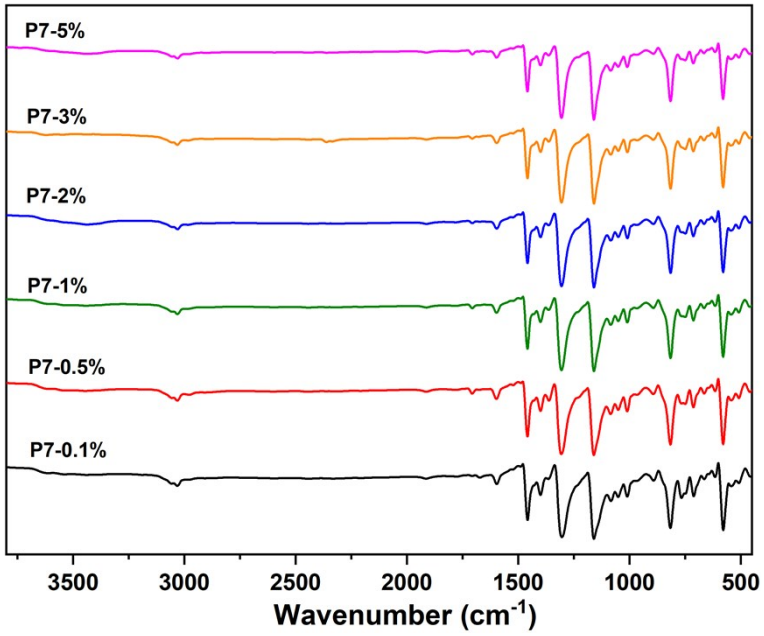

Figure S-8. FT-IR spectra of P7 synthesized with different amouts of [$Pd(PPh_3)_4$].

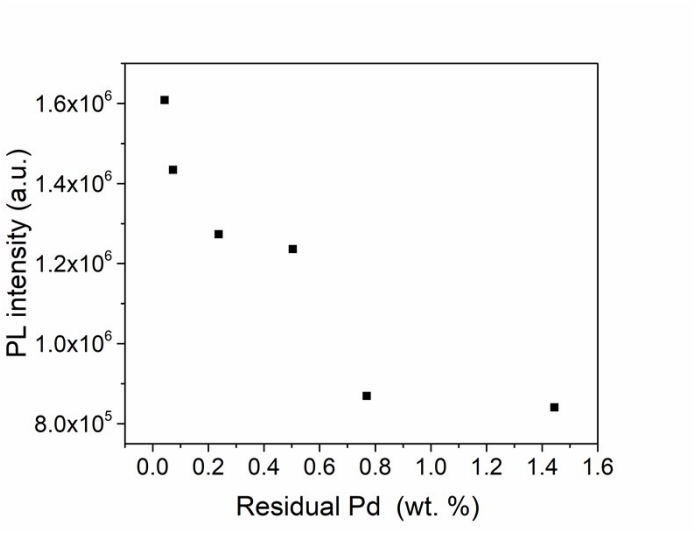

Figure S-9. Photoluminescence intensity (λ_{exc} = 370 nm) of P7 contaning different amounts of residual palladium.

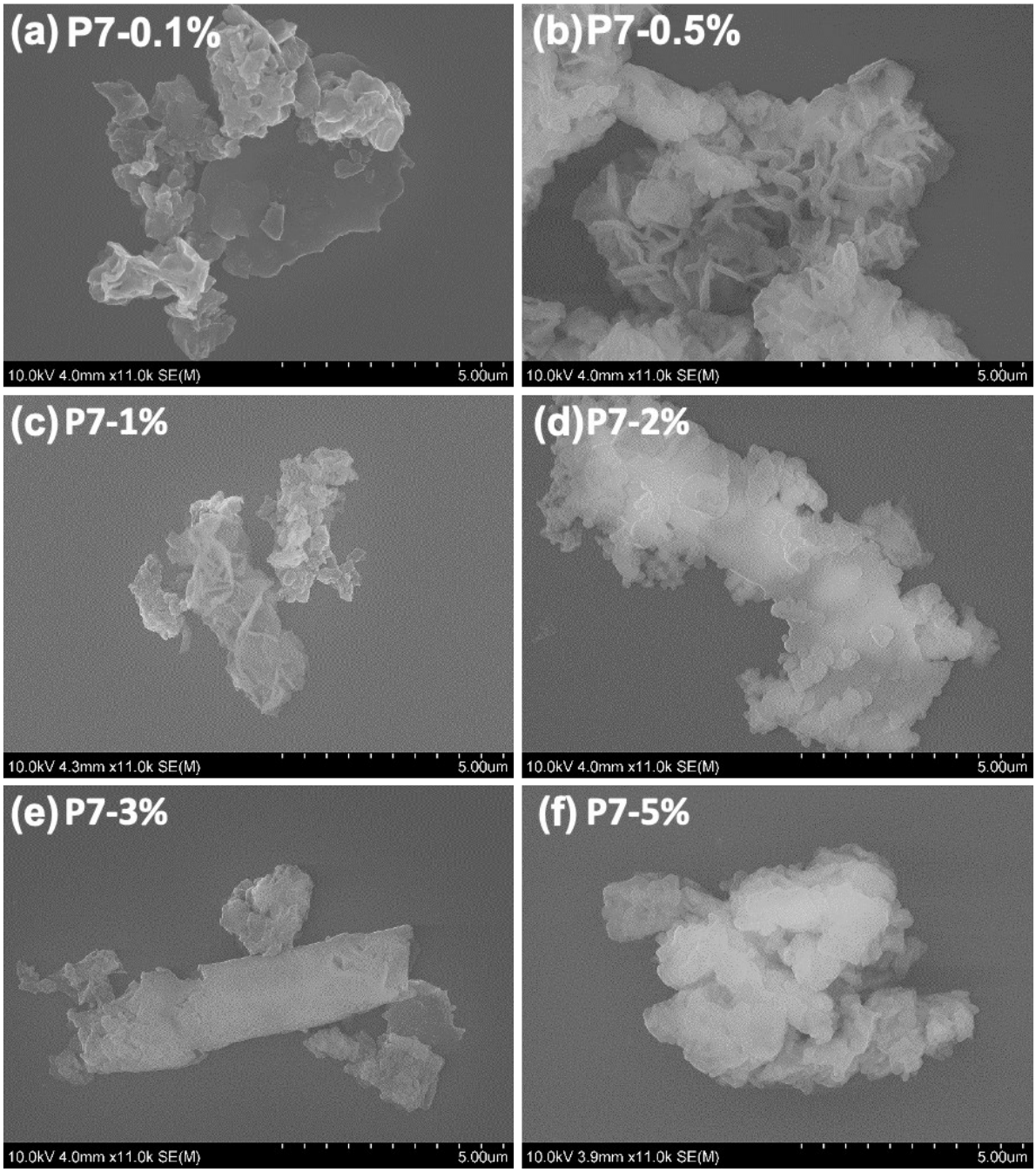

Figure S-10. SEM images of P7 synthesized with different amouts of [$Pd(PPh_3)_4$].

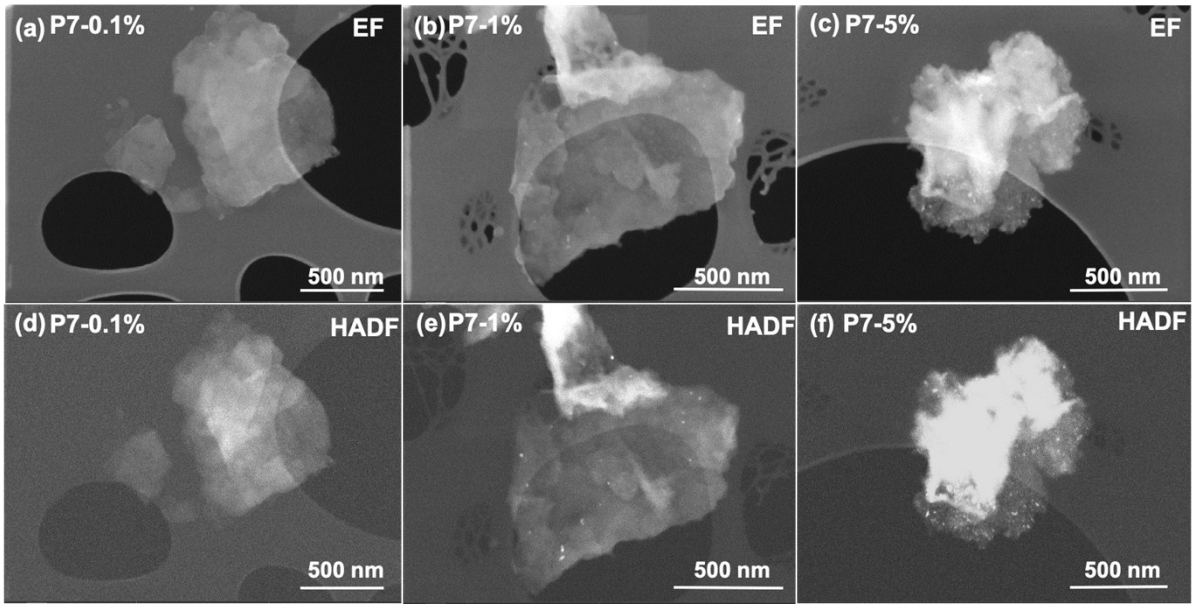

Figure S-11. TEM images of P7-0.1% (a) (d), P7-1% (b) (e), P7-5% (c) (f) using epifluorescent STEM mode and using HADF STEM mode.

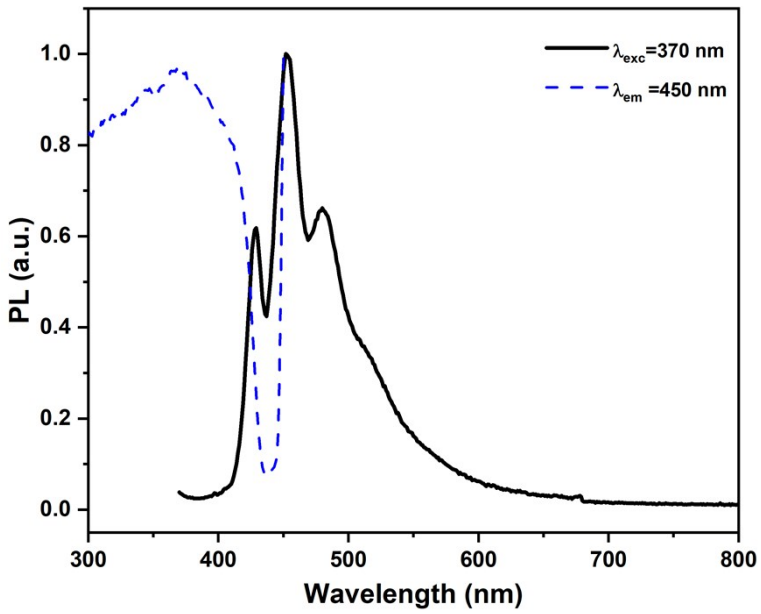

Figure S-12. Fluorescence emission and excitation spectra of **P1** in acetonitrile water and triethanolamine (3/1/1) solution.

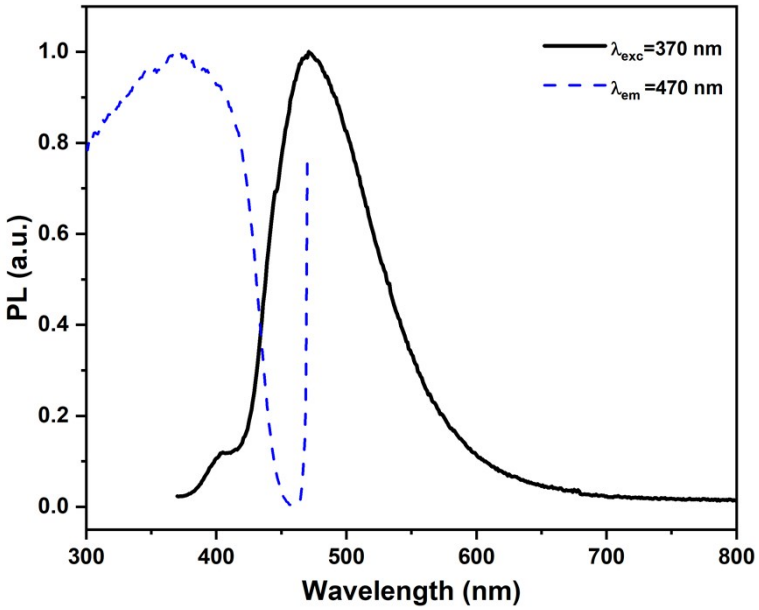

Figure S-13. Fluorescence emission and excitation spectra of **P7** in acetonitrile.

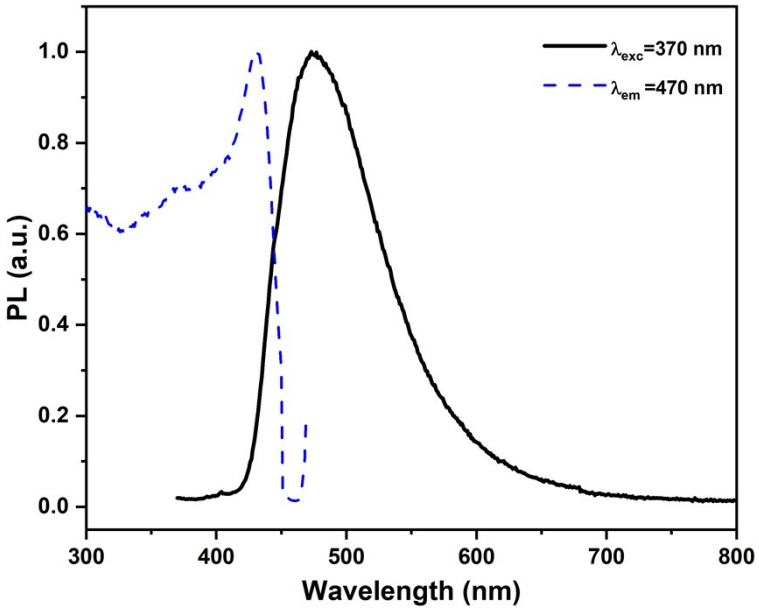

Figure S-14. Fluorescence emission and excitation spectra of **P7** in acetonitrile water and triethanolamine (3/1/1) solution.

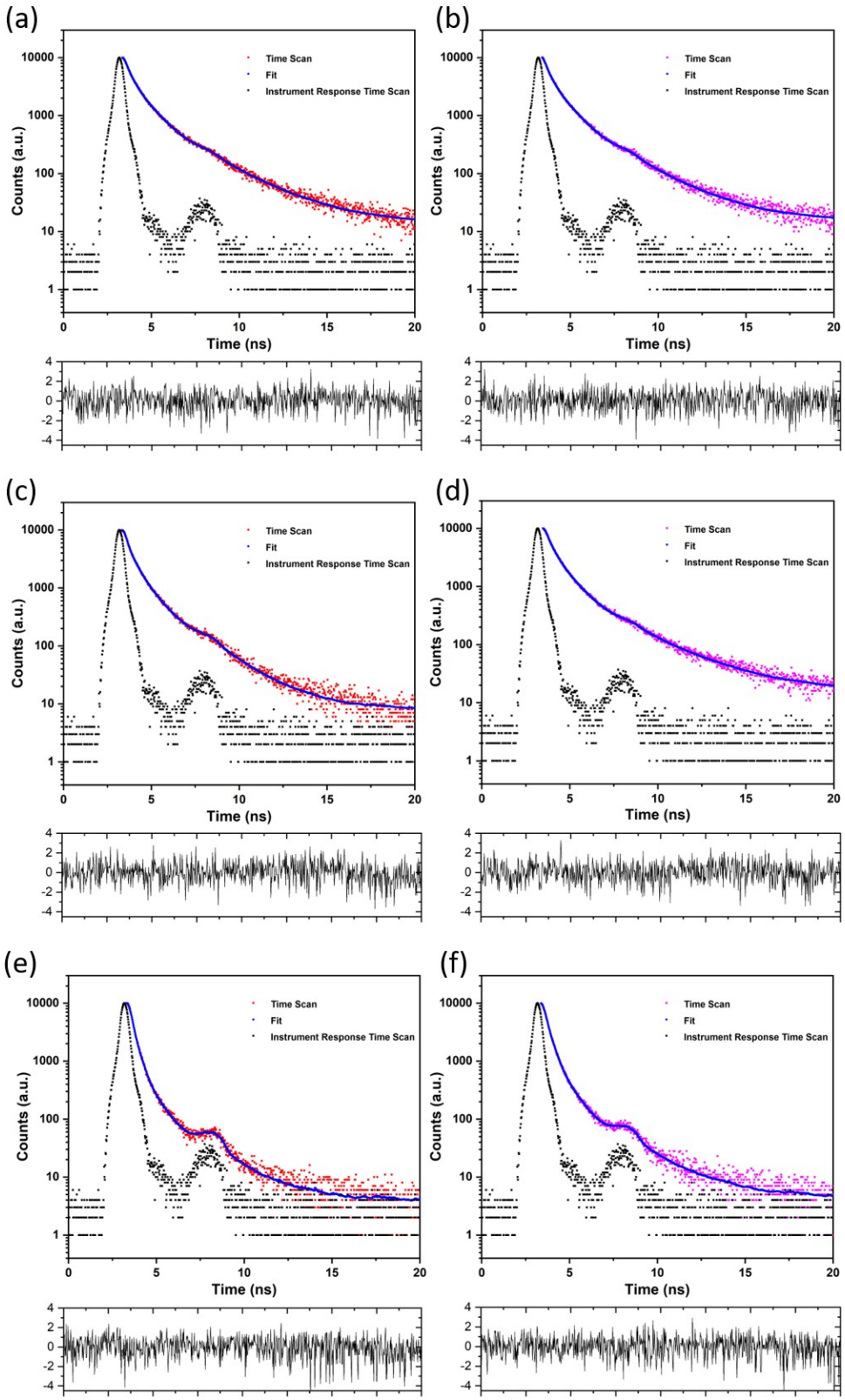

Figure S-15. Fluorescence life-time decays of **P7** in MeCN purged with N_2 (a) or CO_2 (b) and MeCN/H_2O/TEOA (3/1/1) mixture purged with N_2 (c) or CO_2 (d) (λ_{exc} = 370 nm, λ_{em} = 475 nm) and **P1** in MeCN/H_2O/TEOA (3/1/1) mixture purged with N_2 (e) or CO_2 (f) (λ_{exc} = 370 nm, λ_{em} = 450 nm).

Table S-6. Fluorescence life-time measurements.

Materials	λ_{em} / nm	τ_1 / ns	B_1 / %	τ_2 / ns	B_2 / %	τ_3 / ns	B_3 / %	χ^2	τ_{AVG}
P7[a]	475	0.23	31.95	0.91	43.57	2.67	24.48	1.05	1.13
P7[b]	475	0.22	32.06	0.90	43.33	2.57	24.61	1.09	1.05
P7[c]	475	0.14	35.72	0.66	40.89	2.05	23.39	1.10	0.80
P7[d]	475	0.24	30.70	0.89	46.57	2.93	22.73	1.04	1.15
P1[c]	453	0.20	64.04	0.64	27.85	2.35	8.11	1.18	0.50
P1[d]	453	0.16	71.17	0.54	22.05	2.10	6.78	1.28	0.37

[a] Acetonitrile purged with N_2; [b] Acetonitrile purged with CO_2; [c] Acetonitrile water and triethanolamine (3/1/1) purged with N_2; [d] Acetonitrile water and triethanolamine (3/1/1) purged with CO_2.

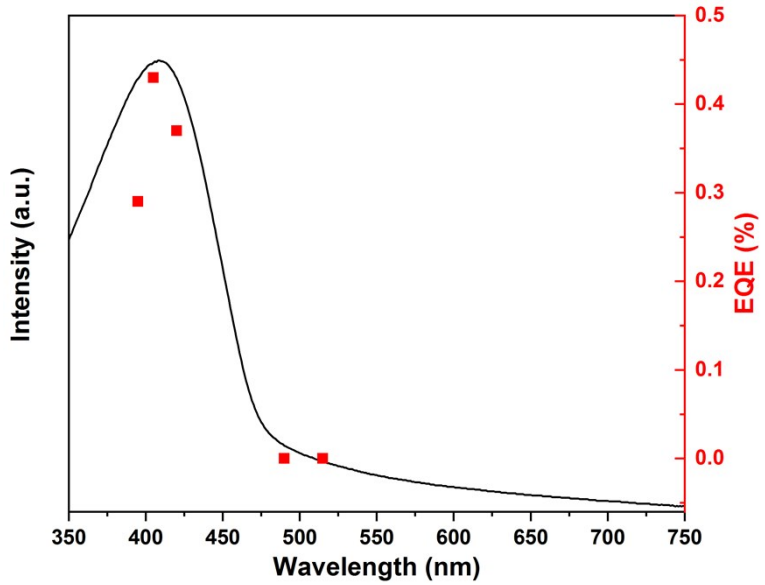

Figure S-16. UV-Vis spectrum of P7-0.1% overlaid with the measured external quantum efficiencies (EQE) measured at various wavelengths using LEDs at light sources.

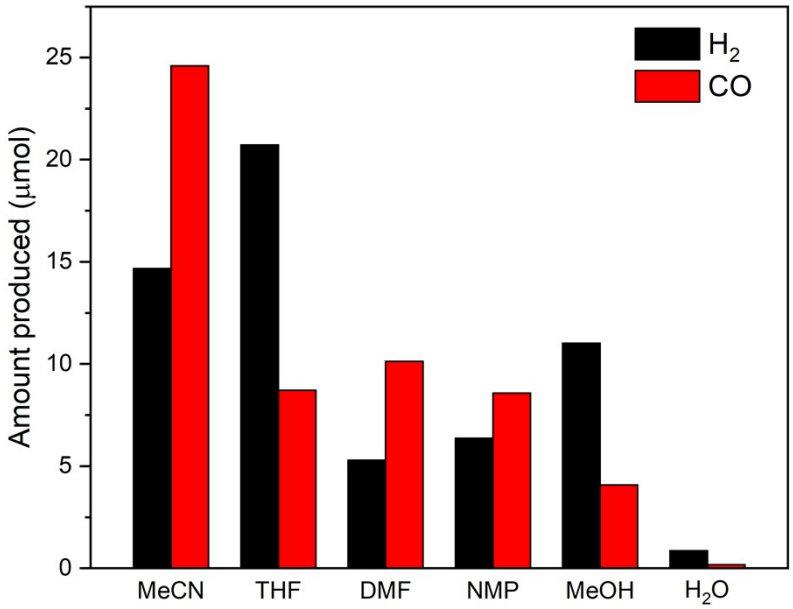

Figure S-17. CO/H_2 production generated using various co-solvents of P7-0.5% as catalyst and 1 mL TEOA as the sacrificial agent under solar simulator irradiation for 5 hours (AM1.5G, 1600 W xenon light source, air mass 1.5G filter, 350−1000 nm); 3 mL Organic solvent and 1 mL water or 4 mL water only (MeCN: acetonitrile; THF: tetrahydrofuran; DMF: *N*,*N*-dimethylformamide; NMP: *N*-methyl-2-pyrrolidone; MeOH: methanol).

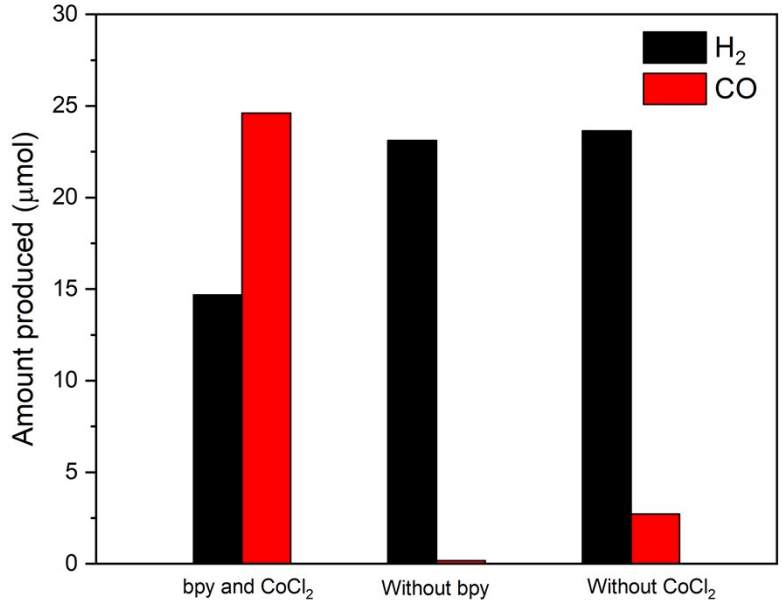

Figure S-18. CO/H_2 production without 2, 2'-bipyridine or $CoCl_2$ using P7-0.5% as catalyst in $MeCN/H_2O$/TEOA mixture (5 mL, 3/1/1) under solar simulator for 5h (AM1.5G, 1600 W xenon light source, air mass 1.5G filter, 350−1000 nm).

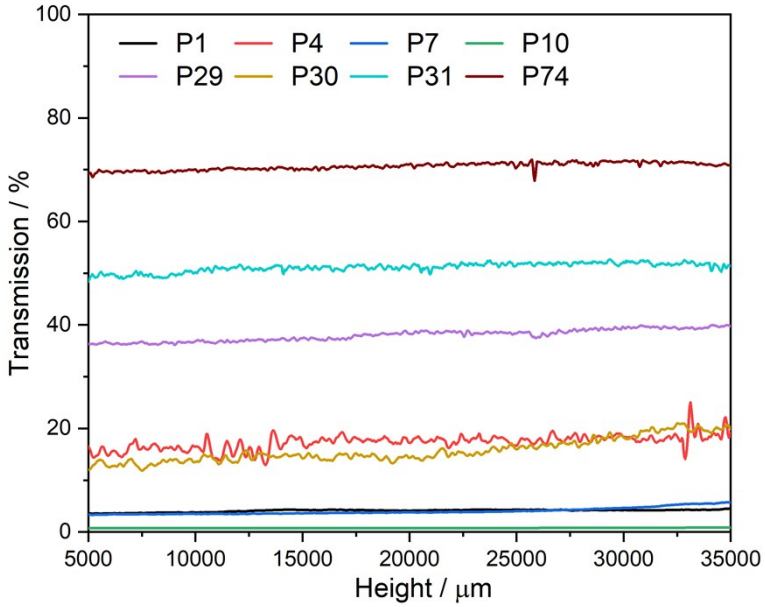

Figure S-19. Transmission experiments of photocatalysts suspended in MeCN/H_2O/TEOA mixture (3/1/1). The transmission of suspensions was measured at 180° relative to the light source.

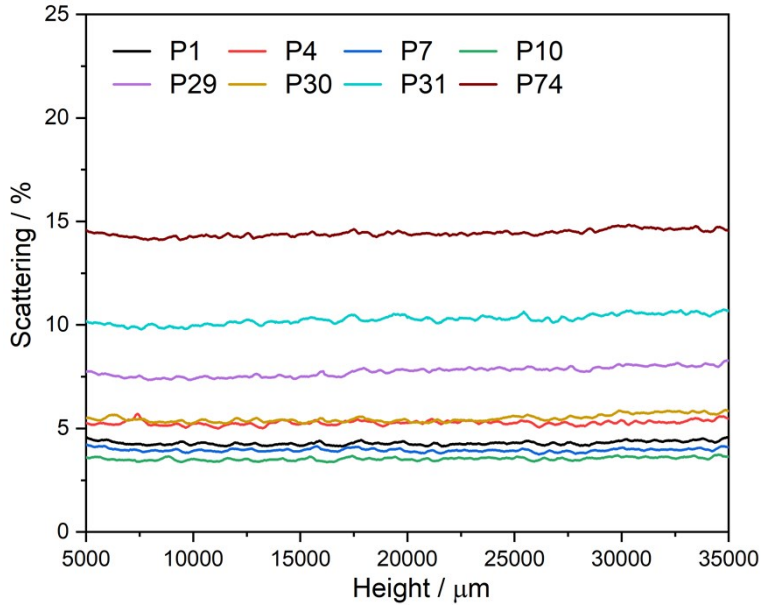

Figure S-20. Backscattering experiments of photocatalysts suspended in MeCN/H_2O/TEOA mixture (3/1/1). The backscattering of the suspensions was measured at 45° relative to the light source.

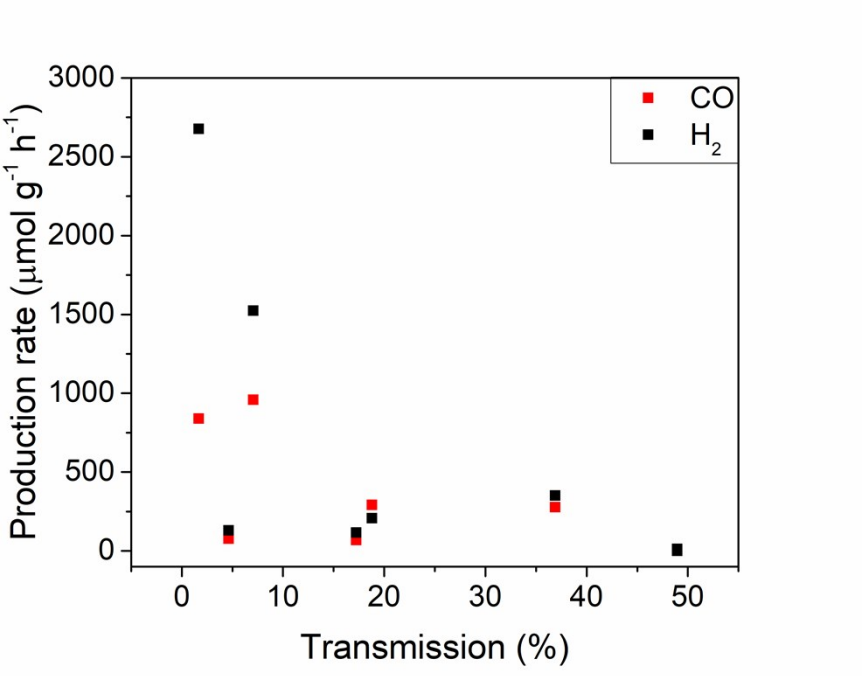

Figure S-21. Average transmission of the photocatalysts suspended in MeCN/H_2O/TEOA mixture (3/1/1) correlated with the observed hydrogen and CO production rates.

Table S-7. IP, EA, IP* and EA* values of polymer P74.

	IP / V	**EA / V**	**IP* / V**	**EA* / V**
P74[a]	0.89	-1.12	-1.17	0.94

[a] Calculated for an oligomer of 12 monomer units long with B3LYP/DZP/COSMO (ε_r 80.1).

Table S-8. Optical properties of photocatalysts.

	Optical gap / eV		
Sexiphenylene	3.45		
P1K	2.74		
P1S	2.74		
P4	2.67		
P7	2.66		
P10S	2.52		
P10Y	2.46		
P29	2.72		
P30	2.61		
P31	2.52		
P74	2.01		

Table S-9. Predicted potentials for charge carriers and exciton in P74 relative to the Standard Hydrogen Electrode.

	E / V
IP	0.89
EA	-1.12
IP*	-1.17
EA*	0.94

Table S-10. Predicted redox solution potentials for the oxidation of TEOA in V at pH 0 and pH 8.3 relative to the Standard Hydrogen Electrode. Potentials calculated under the assumption that oxidation takes places on and near the nitrogen atom rather than one of the OH groups, and that the 2-electron overall oxidation products of TEOA are diethanolamine and 1,1,2-ethanetriol, *i.e.* that the glycolaldehyde formed instantaneously hydrolyses to 1,1,2-ethanetriol.

	E / V	
	pH 0	pH 8.3
DEOA (aq) + ET (aq) + 2 H^+ (aq) + 2 e^- -> TEOA (aq) + 2 H_2O (l)	0.03	-0.46
$TEOA^{\cdot}$ (aq) + H^+ (aq) + e^- -> TEOA (aq)	1.20	0.71
$TEOA^+$ (aq) + e^- -> TEOA (aq)	0.67	0.67

DEOA diethanolamine, ET 1,1,2-ethanetriol, $TEOA^{\cdot}$ triethanolamine radical ($N(CH_2CH_2OH)_2(CH{\cdot}CH_2OH)$).

References

1 P. Guiglion, C. Butchosa and M. A. Zwijnenburg, *J. Mater. Chem. A*, 2014, **2**, 11996–12004.

2 P. Guiglion, A. Monti and M. A. Zwijnenburg, *J. Phys. Chem. C*, 2017, **121**, 1498–1506.

3 C. Lee, W. Yang and R. G. Parr, *Phys. Rev. B*, 1988, **37**, 785–789.

4 A. D. Becke, *J. Chem. Phys.*, 1993, **98**, 5648–5652.

5 P. J. Stephens, F. J. Devlin, C. F. Chabalowski and M. J. Frisch, *J. Phys. Chem.*, 1994, **98**, 11623–11627.

6 A. Schäfer, H. Horn and R. Ahlrichs, *J. Chem. Phys.*, 1992, **97**, 2571–2577.

7 A. Klamt and G. Schüürmann, *J. Chem. Soc., Perkin Trans. 2*, 1993, 799–805.

8 R. S. Sprick, L. Wilbraham, Y. Bai, P. Guiglion, A. Monti, R. Clowes, A. I. Cooper and M. A. Zwijnenburg, *Chem. Mater.*, 2018, **30**, 5733–5742.